Clinical Science (1989) 76, 403-413

Intestinal glucose transport using perfused rat jejunum *in vivo*: model analysis and derivation of corrected kinetic constants

JONATHAN B. MEDDINGS AND HENRIK WESTERGAARD

Department of Internal Medicine, The University of Texas Health Science Center at Dallas, Southwestern Medical School, Dallas, Texas, U.S.A.

(Received 31 December 1987/22 July 1988; accepted 3 August 1988)

SUMMARY

1. The transport model that best describes intestinal glucose transport *in vivo* remains unsettled. Three models have been proposed: (1) a single carrier, (2) a single carrier plus passive diffusion, and (3) a two-carrier system. The objectives of the current studies were to define the transport model that best fits experimental data and to devise methods to obtain the kinetic constants, corrected for diffusion barrier resistance, with this model.

2. Intestinal glucose uptake was measured during perfusion of rat jejunum *in vivo* over a wide range of perfusate concentrations and diffusion barrier resistance was determined under identical experimental conditions. The data were fitted to the transport equations that describe the three models with appropriate diffusion barrier corrections, and the kinetic constants were derived by non-linear regression techniques. The fit of each model to the data was assessed using six statistical tests, five of which favoured a model described by a single carrier and passive diffusion.

3. The main conclusions of these studies are: (1) kinetic constants uncorrected for diffusion barrier resistance are seriously in error; (2) values for the derived kinetic constants are strongly dependent on the transport model selected for the data analysis which underscores the need for rigorous model analysis; (3) corrected kinetic constants may be obtained by either non-linear regression or by a simpler graphical analysis once the correct transport model has been selected and diffusion barrier resistance determined; (4) only corrected kinetic constants should be used for inter-species comparisons or to study the effect of specific interventions on intestinal glucose transport.

Correspondence: Dr Henrik Westergaard, Department of Internal Medicine, The University of Texas, Southwestern Medical Center, 5323 Harry Hines Boulevard, Dallas, TX 75235-9030, U.S.A.

Key words: diffusion barrier resistance, glucose transport, graphical analysis, non-linear regression, statistical analysis.

Abbreviations: Bes,2-[bis-(2-hydroxyethyl)amino]ethanesulphonic acid; Caps, 3-[cyclohexylamino]-1-propanesulphonic acid; Ches, 2-[*N*-cyclohexylamino]ethanesulphonic acid; Hepes, 4-(2-hydroxyethyl)-1-piperazine; Mes, 4-morpholine-ethanesulphonic acid; PEG, polyethylene glycol.

INTRODUCTION

It has become apparent that the intestinal absorption of glucose can be modulated by experimental interventions such as carbohydrate feeding, hyperglycaemia and diabetes, which all appear to increase the maximal velocity of carrier-mediated glucose transport [1, 2]. However, the kinetic interpretation of intestinal glucose transport data is hampered by two major problems. The first of these is the presence of a significant diffusion barrier in the lumen adjacent to the brush-border membrane. This barrier results in the formation of a glucose concentration gradient such that the concentration of glucose at the microvillus membrane may be much less than the concentration of glucose in the perfusate [3, 4]. Under these conditions, classical kinetic analysis, based upon the measured perfusate glucose concentration, leads to erroneous estimation of the kinetic parameters describing the rate of glucose transport [5]. The disparity among published K_m values for intestinal glucose transport may be almost entirely accounted for by the failure to correct for diffusion barrier effects [6]. Thus, in order to define the effects of an experimental intervention on the intestinal glucose transport system accurately, it is imperative that diffusion barrier resistance be accounted for. Several methods are now available to measure the resistance of these barriers [7, 8].

The second problem concerns the actual mechanism of glucose absorption. It is well-documented that the movement of glucose across the intestinal epithelial cell is facilitated by carrier-mediated transport [9]. Recently, it has been suggested that intestinal glucose transport in the perfused rat intestine may be best described by two concurrent transport processes: carrier-mediated transport and passive permeation [10]. However, there is also evidence suggesting that in some species two distinct populations of glucose carriers with different kinetic constants may exist in the microvillus membrane [11–14]. Thus, three entirely different models have been proposed for intestinal glucose transport: (1) carrier-mediated transport by a single carrier, (2) a single carrier with an additional diffusional pathway, (3) two separate carrier systems with differing kinetic parameters. Since the kinetic constants determined from any experiment are dependent upon the transport model used to analyse the data, it is important that the correct model is chosen. Unfortunately, there are no independent methods available for determining the correct mechanisms involved in the movement of glucose across the intestinal epithelium. Therefore, a variety of statistical methods have recently been proposed to assess the ability of a transport model to describe the experimentally observed rates of uptake [15]. Using these techniques, Gardner & Atkins [16] evaluated 35 data sets relating rates of absorption for either amino acids or sugars to substrate concentration in a variety of experimental preparations. They concluded that a single carrier system without a passive component provides the best fit to the data in the greatest number of cases. However, diffusion resistance was not determined in any of these studies, and hence the data were uncorrected for this resistance which may have skewed the analysis. Therefore, in considering intestinal glucose transport from a perfused loop system, where diffusion barrier resistance is significant, it is still unclear which transport model should be utilized.

The current studies have two major objectives. First, to develop mathematical techniques allowing experimental data to be analysed by any of the three models previously described but, importantly, taking into consideration the effects of diffusion barrier resistance. Secondly, to measure both diffusion barrier resistance and the rates of intestinal glucose absorption over a wide concentration range *in vivo* to rigorously determine which model best describes the experimental data using the statistical methods proposed by Atkins and co-workers [15–19]. The perfused intestinal loop *in vivo* was selected for these studies because this transport model offers distinct advantages over techniques *in vitro* in the study of regulation of intestinal glucose transport by experimental interventions.

METHODS

Chemicals

Unlabelled D- and L-glucose were supplied by Mallinckrodt, Inc. (St Louis, MO, U.S.A.); phenobarbital and fatty acids were obtained from Sigma (St Louis, MO, U.S.A.). D-[U-^{14}C]Glucose, L-[1-^{14}C]glucose and [^{3}H]polyethylene glycol (PEG) were from New England Nuclear (Boston, MA, U.S.A.); [^{14}C]phenobarbital was obtained from Amersham (Arlington Heights, IL, U.S.A.) and ^{14}C-labelled fatty acids were from Pathfinder Laboratories (St Louis, MO, U.S.A.). All other compounds were reagent grade.

Measurement of intestinal uptake

Female Sprague–Dawley rats, maintained on normal rat chow (Wayne Lab Blox) and allowed free access to water, were used in all studies. The rats were kept in light-cycled rooms (dark phase 03.00 to 15.00 h) and perfusion studies were performed in the mid-dark phase of the cycle on unfasted rats weighing 200–225 g. The technical aspects of the perfusion *in vivo* have been described in detail elsewhere [8]. Briefly, the rats were anaesthesized with ether and nembutal, and the small intestine was exposed through a midline incision. A proximal jejunal loop measuring about 15 cm in length was isolated, cannulated with tubing and replaced in the abdominal cavity which was subsequently closed. The tubings were connected with a perfusion chamber in a water bath (37°C), and the perfusate, a modified Krebs–bicarbonate buffer, was recirculated through the isolated intestinal loop by means of a peristaltic pump at a perfusion rate of 5 ml/min. The loop was first perfused for 30 min with buffer alone (pH 7.40), and the perfusate was then exchanged for the experimental solution, i.e. buffer to which unlabelled and labelled probes had been added at appropriate concentrations. [^{3}H]PEG was added in trace quantities as a volume marker to correct for net water movement. The perfusate was recirculated through the intestinal loop for 60 min and duplicate 50 μl samples were taken at 10 min intervals and added to 15 ml of scintillation solution (Ria-Solve II, Research Products International, Mount Prospect, IL, U.S.A.). The ^{3}H and ^{14}C radioactivity was counted in a Beckman LS 6800 with automatic quench correction. The glucose concentrations in the perfusate measured either isotopically or chemically during the perfusion were not significantly different. Thus, there is no evidence for significant back flux of labelled metabolites (lactate, CO_2) to the perfusate during perfusion *in vivo*. The ^{14}C radioactivity (d.p.m./ml) of the probe molecule, corrected for water movement measured with [^{3}H]PEG, was plotted against time, and the slope was obtained by linear regression analysis. The negative slope is the disappearance rate of the probe and the rate of uptake was obtained by dividing the rate of disappearance (in d.p.m./min^{-1} ml^{-1}) by the specific activity of the probe molecule and the length of the perfused loop (cm). The results are expressed in nmol of solute absorbed per min per cm length of intestine (nmol min^{-1} cm^{-1}). Since the concentration of the probe molecule decreases with time during intestinal perfusion, the calculated rates of uptake were assumed to be driven by the log mean concentration of the probe [20, 21]. The rates of uptake as a function of perfusate concentration are depicted using the initial, and not the log mean, concentration for ease of presentation.

Determination of diffusion barrier resistance

The resistance of the diffusion barrier in the perfused rat jejunum *in vivo* was determined by defining diffusion-limited probe molecules as outlined in detail elsewhere [8]. Briefly, two different approaches were used to define the resistance of this barrier. First, the rates of uptake for a homologous series of fatty acids (6:0 to 12:0) were measured over a range of fatty acid concentrations. The rates of uptake for all fatty acids were a linear function of concentration as described before [8, 22] and the slope of this relationship was defined as the apparent permeability coefficient ($*P$) of each fatty acid. As described in the Results section, it can be shown that the rates of uptake for fatty acids 10:0 and 12:0 are diffusion limited. Second, the rate of uptake of phenobarbital was measured at a constant perfusate concentration, 0.25 mmol/l, over a pH range from 10.0 to 5.5. In these studies the Krebs–bicarbonate buffer was substituted with one of the synthetic buffers (Mes, Bes, Hepes, Ches or Caps at 50 mmol/l) depending on the desired pH. The buffer also contained 100 mmol/l NaCl and mannitol was added to maintain iso-osmolarity. The buffers were gassed with nitrogen, and the pH remained constant within the desired value ± 0.2 pH units during intestinal perfusion.

Data analysis

Curve fitting was performed using a commercially available statistical program (Systat) on a microcomputer equipped with a maths co-processor. The analysis was performed by fitting the observed data points directly to the equations describing each model without transformations. For each data set, non-linear regression analysis was performed on multiple occasions using different starting estimates for each parameter. Furthermore, for each model both a Quasi-Newton and Simplex algorithm were used to ensure that identical results were obtained. The iterative analysis employed sought to minimize the residual sum of squares between the observed and predicted values. Since diffusion barrier resistance was measured independently the value of this parameter was fixed in each equation before analysis. The program converged to a reproducible solution for each model requiring 8–28 iterations depending on the model and starting parameters. The three models were constrained to pass through the origin. The derivation of the equations describing each model is presented in the Results section and the Appendix.

RESULTS

Diffusion barrier resistance

By definition, movement of any probe molecule across the diffusion barrier occurs by diffusional forces alone. Thus:

$$J_d = (C_1 - C_2) DS_w/d \quad (1)$$

where J_d represents the rate of diffusion, C_1 and C_2 are the concentration of probe molecules in the perfusate and at the membrane interface, respectively, D represents the aqueous diffusion coefficient for the probe molecule and S_w and d represent the surface area and thickness of the diffusion barrier, respectively. While it is possible to measure values for both S_w and d by independent methods [8], a more accurate estimation of diffusion barrier resistance can be obtained to measuring the ratio d/S_w. This ratio can be calculated from the absorption rate of a diffusion-limited probe molecule [8, 23]. By definition, these compounds have such high membrane permeability coefficients that their rate of uptake is determined almost entirely by the rate of diffusion across the diffusion barrier. Thus the concentration of these compounds at the membrane interface (C_2) approaches zero, and therefore eqn (1) reduces to:

$$J_d = C_1 DS_w/d \quad (2)$$

Since J_d/C_1 equals $*P$, eqn (2) becomes:

$$*P = DS_w/d \quad (3)$$

Thus, values of $*P$ for diffusion-limited compounds are proportional to their aqueous diffusion coefficients, or stated differently, $*P$ divided by D will attain a constant value determined by the resistance of the diffusion barrier. Thus, by measuring the absorption rate of a diffusion-limited probe, it is possible to calculate d/S_w by rearranging eqn (3):

$$\frac{d}{S_w} = \frac{D}{*P} \quad (4)$$

In this study diffusion-limited probes were identified using two techniques. First, rates of uptake for a series of fatty acids of increasing chain length (hexanoic 6:0; octanoic 8:0, nonanoic 9:0, decanoic 10:0 and dodecanoic 12:0) were determined at a perfusion rate of 5 ml/min. The apparent passive permeability coefficients for these fatty acids were divided by their respective diffusion coefficients, and the natural logarithm of this quantity, $\ln *P/D$, was plotted against chain length as shown in Fig. 1. As expected, $\ln *P/D$ is a linear function of chain length for fatty acids 6:0 to 10:0, since the membrane permeability coefficients of these molecules increase in a log linear fashion with the addition of $-CH_2-$ groups [22, 24]. The curve reaches a plateau at fatty acid 10:0, and the values of $\ln *P/D$ for fatty acids 12:0 and 10:0 are identical, indicating that the rates of uptake for these molecules are limited by diffusion barrier resistance under these experimental conditions. The magnitude of the resistance is indicated by the horizontal broken line in Fig. 1. With these data it would be predicted that compounds with membrane permeability coefficients of the same magnitude as fatty acids 10:0 and 12:0 would also be diffusion limited. To test this prediction, the rate of uptake of phenobarbital, a non-polar compound with a high membrane permeability coefficient, was measured [25]. Uptake rates were measured at a constant solute concentration of 0.25 mmol/l over a pH range from 10.0 to 5.5. The quantity $\ln *P/D$ for phenobarbital has been plotted as a function of decreasing pH in Fig. 1. The curve describes a sigmoid function as the

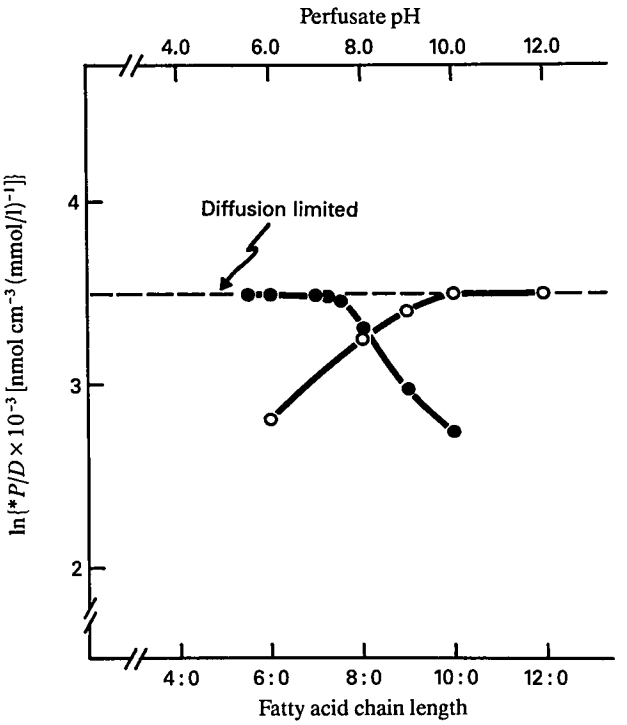

Fig. 1. Fatty acids (○). The apparent permeability coefficients (*P) for fatty acids 6:0, 8:0, 9:0, 10:0 and 12:0 were determined from the slopes of the concentration curves (data not shown) and divided by their respective diffusion coefficients (D). The quantity ln*P/D has been plotted against fatty acid chain length to define diffusion-limited compounds. Phenobarbital (●). The rates of uptake of phenobarbital were measured at a constant solute concentration, 0.25 mmol/l, at different pH values of the perfusate in the pH range from 10.00 to 5.50 as indicated by the upper abscissa. The rates of uptake were converted to apparent permeability coefficients and divided by the diffusion coefficient of phenobarbital. The quantity ln*P/D has been plotted against pH. The horizontal broken line indicates a diffusion-limited situation.

apparent permeability coefficient increases with decreasing pH. The value of ln*P/D reaches a maximum at pH 7.30 and remains constant as the pH of the perfusate is progressively decreased to 5.50. The plateau value is identical with the value determined using fatty acids 10:0 and 12:0 and, therefore, the rate of phenobarbital absorption is diffusion limited at a pH less than or equal to its pK_a (7.30). Thus, three compounds, fatty acids 10:0 and 12:0 and phenobarbital, are diffusion limited under these experimental conditions and permit the determination of diffusion barrier resistance in the perfused rat jejunum *in vivo*. The value of the resistance term (d/S_w) calculated using eqn (4) corresponds to 0.031 ± 0.001 ($n = 26$). The important conclusion of these studies is that it is now possible to calculate the membrane interface concentration of any probe molecule given any perfusate concentration (C_1) by rearranging eqn (1) and using the experimentally determined value of d/S_w:

$$C_2 = C_1 - J_d R \qquad (5)$$

Table 1. Initial and final D-glucose perfusate concentrations

The final perfusate concentrations were determined by means of the known specific activity of D-[^{14}C]glucose in each perfusate. The values for the final concentrations are presented as the mean ± SEM of n observations after perfusion for 60 min.

n	Concn. (mmol/l)	
	Initial	Final
8	5.00	3.99 ± 0.10
9	10.00	8.38 ± 0.10
7	20.00	17.36 ± 0.39
5	30.00	24.96 ± 0.26
10	40.00	34.49 ± 0.30
7	60.00	52.86 ± 0.62
5	80.00	73.48 ± 0.53
6	100.00	92.57 ± 0.66
6	120.00	111.70 ± 0.76

where R now equals d/S_wD, with D representing the diffusion coefficient of the probe molecule selected.

Glucose absorption

D-Glucose uptake was measured over a wide range of perfusate concentrations from 5 to 120 mmol/l. The decrease in D-glucose concentration in the perfusates over a 60 min pefusion period is shown in Table 1 which illustrates the initial and final D-glucose concentrations. The average fall in perfusate concentration was 12% (range 7–18%). The rates of D- and L-glucose uptake as a function of perfusate concentration (C_1) are depicted in Figs. 2(a) and 2(b). Inspection of Fig. 2(a), reveals that this is a curvilinear relationship without a clearly defined maximal rate of uptake. Since there is almost a linear relationship between C_1 and J_d at glucose concentrations greater than 60 mmol/l, it might be suggested that this implies a passive component to total D-glucose transport. A common approach to estimate this passive component is to determine the passive permeability coefficient of glucose from either the slope of the linear part of Fig. 2(a) or by measurement of the rate of uptake of L-glucose (Fig. 2b) which is assumed not to interact with the D-glucose carrier. The apparent permeability coefficients determined with either method yield identical values (2.91 ± 0.14 vs 2.92 ± 0.13 nmol min^{-1} cm^{-1} (mmol/l)$^{-1}$. Many investigators have subtracted the passive component from the total rate of D-glucose transport illustrated by Fig. 2(c), in order to separate the two postulated transport processes. The resulting curve, usually described as the carrier-mediated rate of transport, typically demonstrates saturation kinetics and allows the derivation of the apparent kinetic constants which correspond to a maximal velocity of 280.0 nmol min^{-1} cm^{-1} and a K_m of 13.7 mmol/l. It must be emphasized that this is incorrect and may lead to serious errors in the interpretation of intestinal transport phenomena.

There are two fundamental problems with this approach. The first involves the assumption that a near-

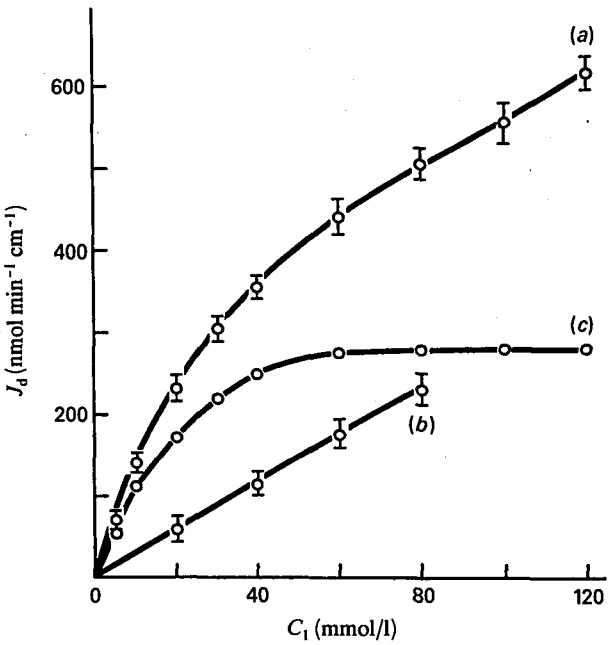

Fig. 2. (*a*) Rates of uptake (J_d) of D-glucose in the perfused rat jejunum *in vivo* as a function of D-glucose concentration in the perfusate (C_1). (*b*) Rate of uptake of L-glucose as a function of L-glucose concentration in the perfusate. Each point represents the mean ± SEM for four to eight rats. (*c*) Calculated difference curve. The curve was obtained by determination of the apparent passive permeability coefficient (*P) for glucose from the slope of (*b*) and subtracting the product *PC_1 from each experimental point in (*a*).

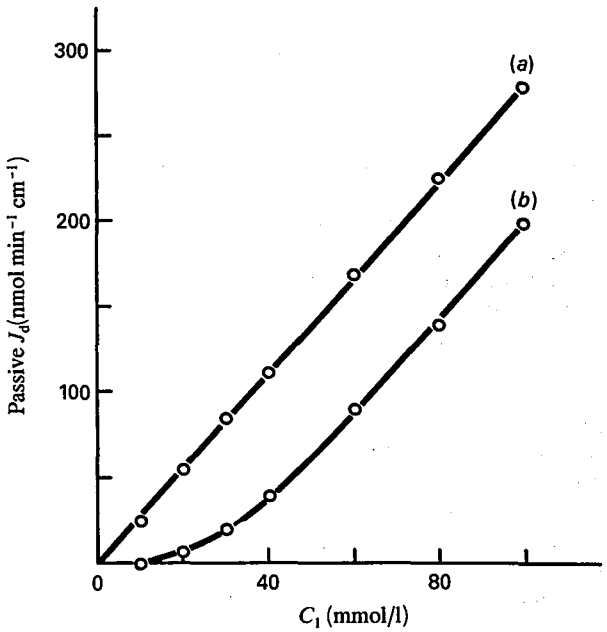

Fig. 3. (*a*) Rates of passive uptake (J_d) of D-glucose in rat jejunum as a function of perfusate concentration (C_1). The *P of D-glucose was obtained from the slope of Fig. 2(*b*), and the points on (*a*) are the calculated products of *PC_1 in the perfusate concentration range. (*b*) The points represent the product PC_2 at each experimental perfusate concentration. The true permeability coefficient (P) for glucose was determined by correction of the apparent permeability coefficient for diffusion barrier resistance, and C_2 was calculated by means of eqn (5) at each perfusate concentration.

linear relationship between J_d and C_1 at high glucose concentrations implies a carrier-independent component to glucose transport. This relationship could be equally well explained by a two-carrier model with differing kinetic parameters. Furthermore, in the presence of a significant diffusion barrier it is possible to observe such a curve with only a single carrier involved in the transport process. Under these conditions, the apparent K_m of the carrier is much higher than the true K_m, and therefore the kinetic curve is displaced towards the right [5]. Thus, if only a relatively narrow concentration range is examined, a curvilinear rather than a saturable kinetic curve would be expected even for the classical model of glucose transport.

The second error in this approach is more subtle [26]. Even if the linear portion of the curve does represent glucose diffusion, simply subtracting this passive component in the presence of a significant diffusion barrier leads to erroneous conclusions. The passive component subtracted is calculated from the apparent permeability coefficient of glucose multiplied by the perfusate glucose concentration (*PC_1) at each experimental point. However, in reality the rate of uptake by this mechanism is determined by the product of the corrected membrane permeability coefficient (P) and the glucose interface concentration (C_2), i.e. PC_2. The difference between the two products as a function of perfusate concentration is illustrated in Fig. 3. It is apparent that *PC_1 exceeds PC_2 at all perfusate concentrations by approximately 1.8-fold. Hence, the product *PC_1 overestimates the passive component to a significant degree, and therefore subtraction of this product from net glucose uptake results in an underestimation of the maximal velocity of the carrier-mediated transport.

Therefore, with these concerns in mind, we proceeded to analyse these data by each of the three previously described models. The mathematical description of each model is as follows:

Model 1: a single membrane carrier alone:

$$J_d = \frac{J^{max.} C_2}{K_m + C_2} \tag{6}$$

Model 2: a single membrane carrier plus a passive component:

$$J_d = \frac{J^{max.} C_2}{K_m + C_2} + PC_2 \tag{7}$$

Model 3: two membrane carriers, a and b, with different kinetic parameters:

$$J_d = \frac{J_a^{max.} C_2}{K_{ma} + C_2} + \frac{J_b^{max.} C_2}{K_{mb} + C_2} \tag{8}$$

In all cases J_d represents the measured rate of glucose uptake; C_2 the interfacial concentration of glucose, $J^{max.}$ the maximal transport velocity, K_m the concentration at which one-half maximal uptake rate occurs and P the corrected membrane permeability coefficient for D-glucose. The experimentally measured parameters are J_d and C_1, and therefore each equation must be solved for J_d after substituting $C_1 - J_d R$ for C_2 (eqn 5). This derivation is presented in the Appendix and the resultant equations describe the rate of glucose uptake (J_d) as a function of the bulk phase glucose concentration (C_1) taking the resistance of the aqueous diffusion barrier (R) into consideration.

The fit of each model to the experimental data was tested as described in the Methods section. In each case the value of R was fixed using the experimentally determined value of d/S_w of 0.031 divided by the diffusion coefficient of D-glucose. Data were entered as either the average rate of uptake at each value of C_1 ($n=9$) or as individual data points ($n=63$). Identical parameter starting values were selected and the program iterated a solution to minimize a LOSS function defined as the residual sum of squares between the observed and predicted uptake rates. Two algorithms were used, the Quasi-Newton and Simplex, and both gave similar results in each case. Furthermore, each model was tested several times using different starting values for the parameters to ensure that both the minimum value of the LOSS function and the parameter estimates were reproducible. The glucose uptake curves as a function of perfusate concentration calculated with the three models are illustrated in Fig. 4 superimposed on the original data points. It is apparent that model 1 provides a poor fit to the data, whereas both model 2 and 3 appear to fit equally well.

After achieving a minimum value for the LOSS function the residuals, defined as:

$$J_d^{observed} - J_d^{predicted}$$

were saved and used in the subsequent statistical anlaysis of each model. These data are presented in Table 2.

The Rankit test evaluates whether the observed residuals are normally distributed. The residuals are ranked from lowest to highest and each is given a Rankit value obtained from a standard table [27]. These are then plotted as a function of the residual value. For normally distributed residuals, a linear relationship is expected. As shown in Table 2, this was only achieved for model 2, and therefore by this criterion model 2 best predicts the observed data.

The second test employed was the Wald-Wolfowitz Runs test [28]. In this test the absolute value of the residuals is ignored. The important parameter is whether the residual has a positive or negative value. Thus, normally distributed residuals would not have long consecutive series of either positive or negative values. The P value reported in Table 2 for this test represents the probability that the residuals are normally distributed by this test. Therefore, the residuals obtained with model 1 probably do not represent a normal distribution, while the residuals from model 2 are more normally distributed than those from model 3.

The third test in Table 2 is a recently described parameter, the Akaike information criterion, that determines a maximal likelihood estimation of the model fitting the observed data [29]. The lower the value of this parameter

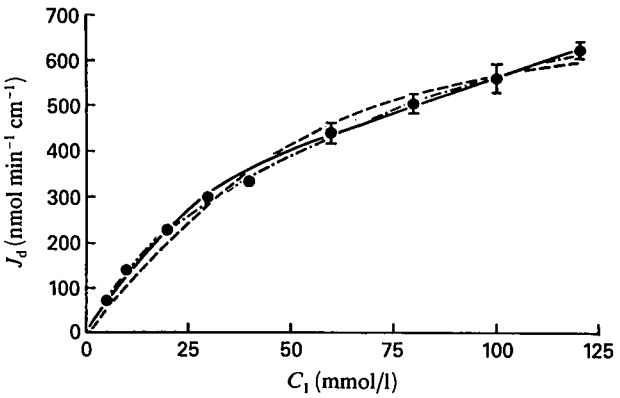

Fig. 4. Goodness of fit of the three models (– – –, model 1; —— model 2; —·—, model 3) to the observed data. The predicted rate of glucose uptake as a function of perfusate concentration was calculated for each of the three models as illustrated by the three lines and superimposed on the original data points (Fig. 2(*a*)).

Table 2. Statistical evaluation of the three mathematical models describing D-glucose absorption

The statistical tests were performed using the mean rate of glucose uptake (J_d) at each experimental perfusate concentration ($n=9$).

Statistical test	Model 1	Model 2	Model 3	
1. Rankit test	Curved	Linear	Curved	
2. Runs test (P)†	0.03	0.66	0.26	
3. Akaike information criterion	80.42	61.77	60.75	
4. Coefficient of variation for each parameter (%)	$K_m=87.2$ $J^{max.}=22.1$	$K_m=29.0$ $J^{max.}=13.0$ $P=22.2$	$K_{ma}=600$ $J_a^{max.}=28.3$	$K_{mb}=728$ $J_b^{max.}=28.5$
5. Speed of convergence	Satisfactory	Satisfactory	Slow	
6. Biological significance	Satisfactory	Satisfactory	Unsatisfactory	

†P, Probability that the residuals are normally distributed.

the better the model fits the experimental data. Thus, by this test, model 1 is a poor description of the relationship between C_1 and J_d, while model 2 and model 3 describe the data equally well.

The coefficient of variation of each parameter estimate can also be used to evaluate which model best fits experimental data. In Table 2 this term is presented as the percentage variation from the mean. Once again, model 2 appears to best represent the experimental situation. Furthermore, the number of iterations required to minimize the LOSS function were much greater with model 3 than either model 1 or 2. Therefore, the convergence to a solution was judged as slow in this model.

Finally, the biological significance of each model was evaluated in light of the final parameter estimates. In order to minimize the LOSS function for model 3, a negative value for the K_m of the first receptor (a) was required and since this is biologically meaningless this model was judged as unsatisfactory.

Thus, in conclusion, these statistical evaluations of the three models overwhelmingly suggest that model 2, with a single carrier and a passive component, best fits the observed data. In no case did either model 1 or model 3 provide a better explanation for the observed rates of glucose absorption than model 2, although by one criterion (the Akaike information criterion) model 3 fits just as well as model 2.

DISCUSSION

The intestinal transport of glucose has been extensively studied in many species with a variety of experimental techniques ranging from isolated microvillus membranes to perfusion of the human small intestine *in vivo*. The determined kinetic constants of the transport process vary widely even within the same species. There are two major reasons for the discrepancy among the published kinetic constants. First, diffusion barrier resistance is significant in most intestinal preparations used in transport studies. Failure to correct for the resistance of these barriers leads to significant errors in the derivation of the kinetic constants [5, 6, 8, 26]. Only in preparations such as isolated intestinal epithelial cells or isolated microvillus membranes, can diffusion barriers be ignored. Second, the derivation of kinetic constants is critically dependent on the transport model used in the kinetic analysis. These constants will be seriously in error if an inappropriate model is used. Three transport models have been proposed for intestinal glucose uptake. Initially, it was assumed that glucose transport was mediated by a single carrier in the microvillus membrane, and the experimental data were fitted to the Michaelis–Menten equation [15]. Secondly, recent observations have been compatible with a model that includes both carrier-mediated and passive permeation [10]. Finally, a third model that included two sets of carriers in the microvillus membrane has been proposed [11–14]. Atkins & Gardner [16] analysed 35 published data sets concerning intestinal glucose and amino acid transport and assessed the ability of each model to explain the experimental data using non-linear regression analysis. The conclusion of this analysis was that a good fit was obtained in only a limited number of cases and that model 1 with a single carrier was the best fit in most cases. It should be emphasized that diffusion barrier resistance was not determined in any of the 35 data sets and consequently only the apparent kinetic constants could be derived. Currently, intestinal glucose transport data, corrected for diffusion barrier resistance, has not been tested for goodness of fit to the proposed transport models by a rigorous analysis.

The current analysis of intestinal glucose transport in the perfused rat jejunum *in vivo*, where glucose uptake and diffusion barrier resistance were measured under identical experimental conditions, provides strong evidence that model 2 with both carrier-mediated and passive pathways best describes the experimental data. This conclusion is based on the results of six statistical tests, described in Table 2, five of which favoured model 2. The conclusion is also corroborated by the fact that only a single protein has been identified as the sodium–glucose transporter in the rabbit microvillus membrane [30, 31]. The evidence for two glucose carriers was obtained by kinetic analysis of glucose transport into microvillus membrane vesicles [11–14]. It is possible that the second carrier represents an artefact of the isolation procedures of the microvillus membranes.

The corrected kinetic constants derived by non-linear regression analysis of the three models are shown in Table 3. The values of the constants in each model, whether derived from the mean J_d or the individual uptake rates, agree reasonably well. However, it should be noted that there is a remarkable difference in the values of $J^{max.}$ and K_m between the three models. The maximal velocity ($J^{max.}$) in model 2 is only 50% of the maximal velocity derived with either model 1 or 3. Similarly, the K_m of the transport process is about 14 mmol/l in model 1 and less than 2 mmol/l in model 2. The fact that K_m is a negative value for one of the carriers of model 3 can be used as a rejection criterion for this model. Hence, both the maximal velocity and K_m will be seriously overestimated if the kinetic analysis is performed with model 1 instead of model 2. The difference in magnitude of the kinetic constants between the three models underscores the need for a careful statistical analysis to select the best fit model.

Since model 2 appears to be the most reasonable explanation of intestinal glucose absorption *in vivo*, it is of interest to compare the kinetic parameters obtained with this model *in vivo* to the kinetic parameters of the glucose carrier defined *in vitro* using isolated intestinal epithelial cells [32]. The latter experimental system has the advantage that diffusion barrier resistance is minimal and therefore kinetic parameters may be obtained by classical techniques. However, it is also clear that the characteristics of the passive diffusion pathway, seen *in vivo*, cannot be examined properly with this preparation. Furthermore, since the units of transport are different in these two preparations, it is difficult to compare maximal transport velocities of the carrier-mediated pathway. However, the K_m value of the carrier should be similar in both experimental preparations. The fact that the K_m for

Table 3. Kinetic parameter estimates obtained by non-linear regression analysis

The three kinetic models for intestinal glucose are described in the Results section, and the equations used in the non-linear regression analysis are outlined in the Appendix. The three kinetic parameters ($J^{max.}$, K_m and P) were derived using either the mean rate of glucose uptake (mean J_d) or the individual rates of uptake at each experimental perfusate concentration. The data are presented as means ± SEM.

Parameter	Model 1		Model 2		Model 3	
	Mean J_d	Individual J_d	Mean J_d	Individual J_d	Mean J_d	Individual J_d
$J^{max.}$ (nmol min^{-1} cm^{-1})	700.7 ± 51.6	703.6 ± 34.5	352.2 ± 15.2	308.2 ± 34.8	a: 195.2 ± 18.4 b: 774.6 ± 73.7	184.5 ± 53.9 700.8 ± 121.3
K_m (mmol/l)	13.8 ± 4	14.1 ± 2.5	1.8 ± 0.2	1.2 ± 0.9	a: −0.07 ± 0.14 b: 63.0 ± 15.3	−0.09 ± 0.37 50.6 ± 3.1
P [nmol min^{-1} cm^{-1} (mmol/l)$^{-1}$]	—	—	3.78 ± 0.28	4.43 ± 0.61	—	—

the glucose carrier measured *in vivo*, with the present techniques, agrees closely with that reported in isolated intestinal cells (~ 1 mmol/l) provides strong support for this method *in vivo*. The additional advantage of the technique *in vivo* is that changes in both the passive component of transport and diffusion barrier resistance can be evaluated simultaneously.

A final point is the interpretation of L-glucose uptake rates. The rates of uptake of L-glucose are considerably lower than those of D-glucose (Fig. 2) and L-glucose uptake is a linear function of perfusate concentration as expected for passive permeation. The notion that L-glucose has a certain affinity to the microvillus D-glucose transporter is not supported by current experimental evidence [9]. Thus, L-glucose should be an excellent probe of the passive permeability of the intestinal epithelium to glucose. The corrected passive permeability coefficient of D-glucose was found to be 3.78 ± 0.28 nmol min^{-1} cm^{-1} (mmol/l)$^{-1}$ using model 2 as the correct model (Table 3). The apparent permeability coefficient (*P) for L-glucose, determined from the data in Fig. 2, equals 2.91 ± 0.14 nmol min^{-1} cm^{-1} (mmol/l)$^{-1}$. When this value is corrected for diffusion barrier resistance the true permeability coefficient is obtained and corresponds to 3.71 ± 0.23 nmol min^{-1} cm^{-1} (mmol/l)$^{-1}$. Thus, the corrected passive permeability coefficients for D-glucose and L-glucose are essentially identical. This observation provides additional support for model 2 as the correct model.

While it is generally recognized that non-linear regression techniques are the most accurate methods available for kinetic parameter estimation [16, 18], it is also possible to analyse such data by simpler graphical methods. However, a prerequisite for these methods is that the appropriate transport model be defined previously. In this example, model 2 represents the appropriate model for intestinal glucose absorption. Since diffusion barrier resistance has been measured, it is possible using eqn (5) to calculate the interfacial concentration of glucose (C_2) for every value of C_1. By replotting the experimental data shown in Fig. 2 as a function of C_2, it is possible to determine the corrected $J^{max.}$, K_m and P as illustrated in the following analysis. Furthermore, this analysis provides a graphical illustration of the effect of diffusion barrier resistance under these experimental conditions. D-Glucose uptake rates plotted as a function of C_2 are shown in Fig. 5 (*a*). This curve has a very steep increase at low glucose concentrations and a more shallow but linear increase at higher concentrations. Fig. 5(*b*) corresponds to Fig. 2(*a*), which has been included for comparison to illustrate the effect of diffusion barrier resistance on net glucose uptake. It is not generally appreciated that the rate of uptake of water-soluble molecules such as D-glucose are affected by this resistance, but as seen in Fig. 5, an appreciable concentration gradient develops across the diffusion barrier. The magnitude of this concentration gradient ($C_1 - C_2$) is indicated by the horizontal distance between the two curves.

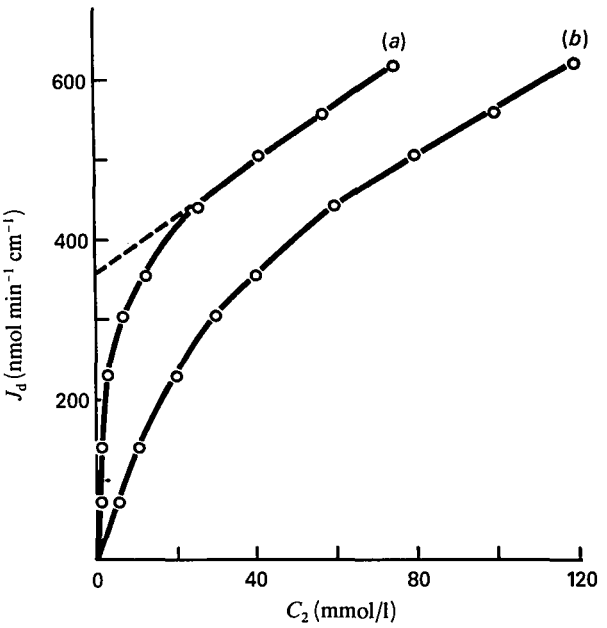

Fig. 5. (*a*) Rates of uptake of D-glucose in rat jejunum as a function of D-glucose concentration at the membrane interface (C_2). The broken line is the slope of the linear portion of (*a*) obtained by linear regression analysis. (*b*) Rate of uptake of D-glucose in rat jejunum as a function of perfusate concentration (C_1). (*b*) is identical with Fig. 2(*a*).

Table 4. Comparison of apparent and corrected kinetic parameters of intestinal glucose transport *in vivo*

The apparent constants were derived by graphical analysis of Fig. 2. The corrected constants were derived by either non-linear regression (Table 2, third column) or by graphical analysis of Fig. 5.

Parameter	Apparent	Corrected	
		Non-linear regression	Graphical analysis
$J^{max.}$ (nmol min^{-1} cm^{-1})	280.0	352.2 ± 15.2	349.2 ± 0.4
K_m (mmol/l)	13.7	1.8 ± 0.2	0.80
P [nmol min^{-1} cm^{-1} $(mmol/l)^{-1}$]	2.92	3.78 ± 0.28	3.65 ± 0.02

The advantage of plotting D-glucose uptake rates as a function of C_2 rather than C_1 is that the corrected passive permeability coefficient (P) and maximal velocity ($J^{max.}$) can be determined from the linear portion of Fig. 5(b) at high C_2 concentrations. The slope of this line (J_d/C_2), determined by linear regression analysis, is equal to the corrected P and corresponds to 3.65 ± 0.02 $nmol^{-1}$ min^{-1} cm^{-1} $(mmol/l)^{-1}$. Furthermore, the intercept of this line on the y-axis, indicated by the broken line, represents the corrected $J^{max.}$ and amounts to 349.2 ± 0.4 nmol min^{-1} cm^{-1}. Once $J^{max.}$ is defined it is possible to obtain K_m graphically simply by interpolation. The interfacial glucose concentration (C_2) required to obtain one-half maximal uptake rate (K_m) approximates 0.8 mmol/l. The corrected kinetic constants of model 2 derived by either non-linear regression or graphical analysis are compared in Table 4 using the mean values of J_d. It is evident that the kinetic parameters derived by either method are in close agreement. The apparent kinetic constants, derived from Fig. 2, i.e. with a correct model but uncorrected for diffusion barrier resistance, have been included in this Table to illustrate the significant disparity between uncorrected and corrected constants.

Therefore, it is now possible to mathematically analyse intestinal transport data obtained *in vivo*, under circumstances where diffusion barrier resistance is significant. The original equations that define transport under these conditions have been extended to include carrier-mediated pathways, diffusional pathways and combinations of both. Furthermore, using several previously described statistical procedures, that evaluate the ability of a mathematical model to predict experimental observations, these studies demonstrate that intestinal glucose absorption from perfused rat jejunum is best explained by a combination of carrier-mediated and passive permeation mechanisms. This conclusion differs from those of several previous investigators [16]. However, in this study diffusion barrier resistance was carefully measured and the interpretation of the data included the effects of this barrier. Using these techniques the affinity of the glucose carrier was found to be nearly identical with that obtained in isolated cells [32] and, furthermore, the measured passive permeability of L-glucose was identical with that of D-glucose obtained by an independent method.

The kinetic constants derived in this study reflect steady-state rates and not initial rates. However, the fact that the K_m value for intestinal glucose transport *in vivo* is identical with the K_m value for the microvillus glucose transporter determined during initial rate conditions [32] suggests that initial rates and steady-state rates are not significantly different. Furthermore, the close agreement between these determined K_m values would argue that movement of glucose across the microvillus membrane is the rate-limiting step in intestinal glucose absorption. The K_m value for the basolateral glucose transporter determined in isolated vesicles is in the range 40–50 mmol/l [33].

In conclusion, these studies provide a basis for measurements of diffusion barrier resistance and solute transport under identical experiment conditions in the perfused intestinal loop preparation *in vivo* which then allow for a more rigorous data analysis and interpretation. Thus, it is now possible to investigate the regulation of intestinal transport systems under different physiological and pathophysiological conditions.

ACKNOWLEDGMENTS

This work was supported by National Institutes of Health grants HL-09610 and M-19329, and by grants from the Moss Heart Foundation, the Texas Affiliate of the American Heart Association and the Diabetes Research and Education Foundation. J.B.M. was supported by the Alberta Heritage Foundation.

REFERENCES

1. Diamond, J.M. & Karasov, W.H. (1984) Effect of dietary carbohydrate on monosaccharide uptake by mouse small intestine *in vivo*. *Journal of Physiology (London)*, **349**, 419–440.
2. Csaky, T.Z. & Fischer, E. (1981) Intestinal sugar transport in experimental diabetes. *Diabetes*, **30**, 568–574.
3. Dietschy, J.M. (1978) Effect of diffusion barriers on solute uptake into biological systems. In: *Microenvironments and Metabolic Compartmentation*, pp. 401–418. Ed. S'rere, P.A. & Estabrook, R.W. Academic Press, New York.
4. Winne, D. (1973) Unstirred layer, source of biased Michaelis constant in membrane transport. *Biochimica et Biophysica Acta*, **298**, 27–31.

5. Thomson, A.B.R. & Dietschy, J.M. (1977) Derivation of the equations that describe the effects of unstirred water layers on the kinetic parameters of active transport processes in the intestine. *Journal of Theoretical Biology*, **64**, 277–294.
6. Barry, P.H. & Diamond, J.M. (1984) Effects of unstirred layers on membrane phenomena. *Physiological Reviews*, **64**, 763–872.
7. Levitt, M.D., Aufderheide, T., Fetzer, C.A., Bond, J.H. & Levitt, D.G. (1984) Use of carbon monoxide to measure luminal stirring in the rat gut. *Journal of Clinical Investigation*, **74**, 2056–2064.
8. Westergaard, H., Holtermuller, K.H. & Dietschy, J.M. (1986) Measurement of resistance of barriers to solute transport *in vivo* in rat jejunum. *American Journal of Physiology*, **250**, G727–G735.
9. Hopfer, U. (1987) Membrane transport mechanisms for hexoses and amino acids in the small intestine. In: *Physiology of the Gastrointestinal Tract*, vol. 2, pp. 1499–1526. Ed. Johnson, L.R. Raven Press, New York, 1987.
10. Debnam, E.S. & Levin, R.J. (1975) An experimental method of identifying and quantifying the active transfer electrogenic component from the diffusive component during sugar absorption measured *in vivo*. *Journal of Physiology (London)*, **246**, 181–196.
11. Honneger, P. & Semenza, G. (1973) Multiplicity of carriers for free glucalogues in hamster small intestine. *Biochimica et Biophysica Acta*, **318**, 390–410.
12. Kaunitz, J.D. & Wright, E.M. (1984) Kinetics of sodium D-glucose cotransport in bovine intestinal brush border vesicles. *Journal of Membrane Biology*, **79**, 41–51.
13. Freeman, H.J. & Quamme, G.A. (1980) Age-related changes in sodium-dependent glucose transport in rat small intestine. *American Journal of Physiology*, **251**, G208–G217.
14. Solberg, D.H. & Diamond, J.M. (1987) Comparison of different dietary sugars as inducers of intestinal sugar transporters. *American Journal of Physiology*, **15**, G574–G591.
15. Atkins, G.L. & Gardner, M.L.G. (1977) The computation of saturable and linear components of intestinal and other transport kinetics. *Biochimica et Biophysica Acta*, **468**, 127–145.
16. Gardner, M.L.G. & Atkins, G.L. (1982) Kinetic analysis of transport processes in the intestine and other tissues. *Clinical Science*, **63**, 405–414.
17. Atkins, G.L. (1983) A comparison of methods for estimating the kinetic parameters of two simple types of transport process. *Biochimica et Biophysica Acta*, **732**, 455–463.
18. Atkins, G.L. (1976) Tests for the goodness of fit of models. *Biochemical Society Transactions*, **4**, 357–361.
19. Nimmo, I.A. & Atkins, G.L. (1976) Methods for fitting equations with two or more non-linear parameters. *Biochemical Journal*, **157**, 489–492.
20. Atkins, G.L. (1981) Mean solute concentration for use with the Michaelis–Menten equation applied to the analysis of data from intestinal perfusion experiments. *Biochemica et Biophysica Acta*, **649**, 143–145.
21. Winne, D. & Markgraf, I. (1979) The longitudinal intraluminal concentration gradient in the perfused rat jejunum and the appropriate mean concentration for calculation of the absorption rate. *Naunyn-Schmiedeberg's Archives of Pharmacology*, **309**, 271–279.
22. Westergaard, H. (1987) The passive permeability properties of *in vivo* perfused rat jejunum. *Biochimica et Biophysica Acta*, **900**, 129–138.
23. Westergaard, H. & Dietschy, J.M. (1974) Delineation of the dimensions and permeability characteristics of the two major diffusion barriers to passive mucosal uptake in the rabbit intestine. *Journal of Clinical Investigation*, **54**, 718–732.
24. Diamond, J.M. & Wright, E.M. (1969) Molecular forces governing nonelectrolyte permeation through cell membranes. *Proceedings of the Royal Society of London, Series B: Biological Sciences*, **172**, 273–316.
25. Jackson, M.J., Williamson, A.M., Dombrowski, W.A. & Garner, D.E. (1978) Intestinal transport of weak electrolytes. Determinants of influx at the luminal surface. *Journal of General Physiology*, **71**, 301–327.
26. Spady, D.K., Meddings, J.B. & Dietschy, J.M. (1986) Kinetic constants for receptor-dependent and receptor-independent low density lipoprotein transport in the tissues of the rat and hamster. *Journal of Clinical Investigation*, **77**, 1474–1481.
27. Harter, H.L. (1961) Expected values of normal order statistics. *Biometrika*, **48**, 151–163.
28. Wald, A. & Wolfowitz, J. (1940) On a test of whether two samples are from the same population. *Annals of Mathematics and Statistics*, **11**, 147–162.
29. Yamaoka, K., Nakagawa, T. & Uno, T. (1977) Application of Akaike's information criterion (AIC) in the evaluation of linear pharmacokinetic equations. *Journal of Pharmacokinetics and Biopharmaceutics*, **6**, 165–175.
30. Schmidt, U.M., Eddy, B., Fraser, C.M., Venter, J.C. & Semenza, G. (1983) Isolation of (a subunit of) the Na^+/D-glucose cotransporter(s) of rabbit intestinal brush border membranes using monocloncal antibodies. *FEBS Letters*, **161**, 279–283.
31. Peerce, B.E. & Wright, E.M. (1984) Sodium-induced conformational changes in the glucose transporter of intestinal brush borders. *Journal of Biological Chemistry*, **259**, 14105–14112.
32. Kimmich, G.A. (1979) Intestinal transport: studies with isolated epithelial cells. *Environmental Health Perspectives*, **33**, 37–44.
33. Maenz, D.D. & Cheeseman, C.I. (1987) The Na^+-independent D-glucose transporter in the enterocyte basolateral membrane. *Journal of Membrane Biology*, **97**, 259–266.

APPENDIX

The equations that describe the three models can be derived as follows using the symbols as previously defined.

1. Model 1: a single carrier located in the brush-border membrane. Therefore:

$$J_d = \frac{J^{max.} C_2}{K_m + C_2} \tag{9}$$

Since $C_2 = C_1 - J_d R$ (eqn 5), substituting for C_2 yields:

$$J_d = \{-K_m - C_1 - J^{max.} R) + [K_m + C_1 + J^{max.} R)^2 - 4RJ^{max.} C_1]^{1/2}\}/-2R \tag{10}$$

2. Model 2: a single carrier located in the brush-border membrane with a passive component determined by a true membrane permeability coefficient (P):

$$J_d = \frac{J^{max.} C_2}{K_m + C_2} + PC_2 \tag{11}$$

Again, substitution for C_2 yields the following relationship:

$$J_d = \{K_m + C_1 + J^{max.} R + 2PRC_1 + PRK_m) + [(K_m + C_1 + J^{max.} R + 2PCR + PRK_m)^2 - 4(R + PR^2)(J^{max.} C_1 + PC_1 K_m + PC^2)]\}/-2R - 2PR^2 \tag{12}$$

3. Model 3: two distinct carriers located in the brush-border membrane denoted carrier a and carrier b:

$$J_d = \frac{J_a^{max.} C_2}{K_{ma} + C_2} + \frac{J_b^{max.} C_2}{K_{mb} + C_2} \tag{13}$$

Substitution for C_2 in this case results in a cubic equation that has three real distinct roots. This can be demonstrated by reorganizing eqn (5) into the form:

$$AJ_d^3 + BJ_d^2 + CJ_d + D = 0 \tag{14}$$

Under these circumstances:

$$A = R^2$$

$$B = (-2RC_1 - RK_{mb} - K_{ma}R - J_a^{max.}R^2 - J_b^{max.}R^2)$$

$$C = (C_1^2 + K_{mb}C_1 + K_{ma}C_1 + K_{ma}K_{mb} + 2J_a^{max.}C_1R + J_a^{max.}RK_{mb} + 2J_b^{max.}C_1R + J_b^{max.}RK_{ma})$$

$$D = (-J_a^{max.}C_1K_{mb} - J_a^{max.}C_1^2 - J_b^{max.}C_1K_{ma} - J_b^{max.}C_1^2)$$

Dividing both sides by A, to eliminate this term, let

$$H = B/A$$

$$I = C/A$$

$$S = D/A$$

Therefore

$$J_d^3 + HJ_d^2 + IJ_d + S = 0$$

Next to remove the square term, let

$$T = (H/3)^2 - (I/3)$$

$$U = -(H/3)^2 + (HI/6) - (S/2)$$

$$V = T^2 - U^3$$

Since $V < 0$ for physiologically reasonable values of the parameters, there exist three different real roots to this problem [1]. Upon inspection of these values only one provides a reasonable solution and may be found as follows. Let

$$\alpha = \arctan[(T^3/U^2 - 1)^{1/2}]$$

and

$$J_d = [2(T)^{\alpha}\cos(\tfrac{1}{2}/3 + 2\pi/3)] - H/3 \tag{15}$$

REFERENCE

1. Bronshtein, I.N. & Semendyayev, K.A. (1978) Algebraic equations. *Handbook of Mathematics,* pp. 120–121. Van Nostrand Reinhold Company, New York.